

Title	Seabed image acquisition and survey design for cold water coral mound characterisation
Authors	Lim, Aaron;Kane, Adam;Arnaubec, Aurélien;Wheeler, Andrew J.
Publication date	2017-09-28
Original Citation	Lim, A., Kane, A., Arnaubec, A. and Wheeler, A. J. (2017) 'Seabed image acquisition and survey design for cold water coral mound characterisation', Marine Geology, 395, pp. 22-32. doi:10.1016/j.margeo.2017.09.008
Type of publication	Article (peer-reviewed)
Link to publisher's version	10.1016/j.margeo.2017.09.008
Rights	© 2017, Elsevier B.V. All rights reserved. This manuscript version is made available under the CC-BY-NC-ND 4.0 license. - http://creativecommons.org/licenses/by-nc-nd/4.0/
Download date	2024-05-07 08:23:30
Item downloaded from	https://hdl.handle.net/10468/5199



UCC

University College Cork, Ireland
 Coláiste na hOllscoile Corcaigh

Seabed image acquisition and survey design for cold water coral mound characterisation

Aaron Lim^{*1), 3)}, Adam Kane¹⁾, Aurélien Arnaubec²⁾ and Andrew J. Wheeler^{1), 3)}

¹⁾ School of Biological, Earth and Environmental Sciences, University College Cork, Distillery Fields, North Mall, Cork, Ireland

²⁾Unité Systèmes sous-Marins, Centre de Méditerranée, Ifremer, Zone Portuaire de Brégaillon, CS 20330, 83507 La Seyne/Mer Cedex, France

³⁾ Irish Centre for Research in Applied Geosciences, University College Cork, Ireland

*Corresponding author: aaron.lim@ucc.ie

Keywords: cold water corals, mounds, video survey design, sediments, habitat mapping

Abstract

Cold-water coral (CWC) habitats are commonly regarded as hotspots of biodiversity in the deep-sea. However, a standardised approach to monitoring the effects of climate change, anthropogenic impact and natural variability through video-surveying on these habitats is poorly-established. This study is the first attempt at standardising a cost-effective video-survey design specific to small CWC mounds in order to accurately determine the proportion of facies across their surface. The Piddington Mound of the Moira Mounds, Porcupine Seabight, offshore Ireland has been entirely imaged by downward-facing video in 2011 and 2015. The 2011 video data is navigated into a full-mound, georeferenced video mosaic. A quadrat-based manual classification of this video mosaic at 0.25 m² resolution shows the exact proportion of facies abundance across the mound surface. The minimum number of random downward-facing images from the mound are determined to accurately characterise mound surface facies proportions. This minimum sample size is used to test the effectiveness of various common

survey designs for ROV-video-based habitat investigations. Single-pass video lines are not representative of the mound surface whilst gridded survey designs yield best results, similar to 100% mound coverage. The minimum sample size and manual classification are applied to the 2015 video data to show a 19% mound surface facies change over 4 years at 0.25 m² resolution. The proportion of live coral facies show little change while coral rubble facies show most change. This highlights an inconsistency between temporally-separated data sets and implies that in 20 years, the mound surface may almost entirely change.

1 Introduction

Cold-water corals (CWC) are sessile, filter-feeding organisms found in many parts of the world's oceans, being common and well-studied in the NE Atlantic (Freiwald, 2002; Roberts et al., 2003; Roberts et al., 2006; Wheeler et al., 2007). Also referred to as “deep-water” corals, their distribution actually covers a large depth range being found from 39 m to 2000 m water depth (Freiwald et al., 2004; Roberts et al., 2006). As their name suggests, they typically exist in cooler waters from 4°C to 13°C (Freiwald, 2002) with the exception of *Oculina* spp., and within a salinity range of 31.7 ‰ - 38.8 ‰ (Davies et al., 2008). *Lophelia pertusa* is the most well-studied framework-forming CWC and is reliant on currents for food supply (Orejas et al., 2016; Purser et al., 2010 and references therein) and can form 3D carbonate structures that benefit from its ability to baffle currents and thereby enhance sedimentation (Wheeler, Kozachenko, et al., 2005; Wheeler et al., 2008). The complex hydrodynamic relationship between the CWC framework, food supply, currents and sedimentation often results in the generation of positive bathymetric features on the seabed called CWC mounds (De Mol et al., 2007; Dorschel, 2003; Squires, 1964; Wilson, 1979). Wilson (1979) and Squires (1964) describe the early-stage development of cold-water coral mounds using evidence from rock outcrop, museum specimens and submersible dives. Through successive and continuous

periods of CWC mound development in the same location, they can generate bathymetric features up to 350 m from base to summit (Henriet et al., 2014 and references therein). Evidence from a number of studies show that the continued development of these coral mounds is largely controlled by environmental conditions (Dullo et al., 2008; Raddatz et al., 2014; Rüggeberg et al., 2007), sediment supply (De Mol et al., 2007; Wheeler, Kozachenko, et al., 2005) and biological processes (Wienberg et al., 2008). Furthermore, a number of mound-development models linked to glacial-interglacial cycles have been presented (Douarin et al., 2014; Eisele et al., 2008; Roberts et al., 2009; Wheeler and Stadnitskaia, 2011).

Advances in marine survey technologies and techniques have fostered novel research opportunities to help better understand the marine environment, particularly in cold-water coral habitats (e.g. Freiwald and Wilson, 1998; Mangini et al., 1998; Mortensen et al., 2001; Roberts et al., 2009). As such, marine remotely-sensed mapping of CWC habitats is becoming progressively more common through the use of side scan sonar (SSS) and multibeam echosounders (MBES). For example, Huvenne et al. (2005) examine the influence of currents and sediment dynamics on the growth of coral and mound development at a mound province scale whereas Dorschel et al. (2009) provide an environmental context to cold-water coral carbonate mound development, both using regional SSS mapping (TOBI 30 kHz SSS). More recently, increased resolution (0.2 m x 0.2 m) SSS surveying has allowed for detailed inspections of coral habitat change in Marine Protected Area's over relatively short timescales (Huvenne et al., 2016). MBES has also proven an integral part of marine habitat mapping for CWC habitats using hull-mounted (Beyer et al., 2003), ROV-mounted (Dolan et al., 2008; Lim et al., 2017), AUV-mounted (Correa et al., 2012) and forward-facing MBES systems (Huvenne et al., 2011).

With recent advances in more accurate underwater positioning for deployed marine sampling/surveying equipment (Chitre et al., 2008; Kinsey et al., 2006), ground-truthing of

marine remotely-sensed mapping coverages is now possible with the effective positioning of still camera and video (ROV and drop frame). ROV video has proven useful in both covering large areas (Guinan et al., 2009; Huvenne et al., 2005) and providing baseline studies (Vertino et al., 2010) within CWC habitats. More recently, techniques for imaging complex structures in difficult, deep-water environments has become better developed at higher resolutions (e.g. Robert et al., 2017).

Temporal variability across CWC habitats has been studied at various scales. Lavaleye et al. (2009) utilize long time-series datasets to understand CWC habitat functioning and its effect on the organic biochemistry of the mound-influencing water column. Anthropogenic impact (trawling activities and drill cutting) at CWC habitats have driven some temporal variability research. However, these studies reveal information about temporal mound surface change utilising different approaches to video inspection at 1, 4 or 10 year timescales (Huvenne et al., 2016; Lundälv et al., 2008; Purser, 2015).

It is now more common to map (bathymetry and backscatter), physically sample (coring and grabs) and image (ROV video) CWC habitats for research purposes. Various combinations of these data types at differing resolutions in different geographic settings, and quite often with a temporal gap between sampling, are utilised to make parallels and contrasts between these habitats. Although not ideal, this is often done due to the costly and time-consuming nature of deep-water data acquisition under weather- and sea state-dependant conditions. However, a common finding of this research is the heterogeneity of these habitats (Lim et al., 2017; Vertino et al., 2010; Wienberg et al., 2009) stressing the need for local-scale studies (Davies and Guinotte, 2011; Dolan et al., 2008; Robert et al., 2016) with a robust sampling density. In light of this, our aim is to identify the minimum amount of imagery needed to accurately quantify the proportion of sediment facies on surface of an individual CWC mound and assess how to best collect this imagery in a representative manner. Furthermore, CWC mounds exist in

dynamic environments but how rapidly do these mounds change? Growth rates of corals give us a clue but how does that translate into full-mound surface change? This study therefore also assesses relative temporal change in mound surface facies and uses this data to assess the temporal consistency of data. However, this method should be corroborated in other areas to assess its robustness.

2 Materials and Methods

2.1 Study Site

The Piddington Mound, a CWC mound in the Belgica Mound Province (BMP), has been selected for this study due to the existence of high-resolution imagery (Video and bathymetry) with sufficient spatial mound coverage as presented in Lim et al. (2017). The BMP is located on the eastern slope of the Porcupine Seabight, NE Atlantic (Fig. 1). Previously designated as a Special Area of Conservation (SAC) under the EU Habitats Directive, the BMP hosts 2 chains of contour-parallel giant CWC carbonate mounds ranging in height from 50 m to 100 m and having a slight elongate to conical morphology (Wheeler, Kozachenko, et al., 2005). A salinity maximum from 600 m to 1000 m water depth marks the depth range of the Mediterranean Outflow Water (MOW), the main mound-influencing water mass in the BMP where intermediate nepheloid layers increase food availability and lateral transport of coral larvae and therefore, influencing their distribution (Dullo et al., 2008; White, 2007).

Between and around these chains of giant CWC carbonate mounds, are approximately 250 CWC mounds, referred to as the “Moirs Mounds” (Wheeler et al., 2011) of which the Piddington Mound is an example. They are small (typically ~10 m tall and 40 m x 60 m in areal extent) with an ovoid to elongate morphology. It is speculated that they are Holocene in age (Huvenne et al., 2005). They exist in various different settings: at the head of sediment wave trains, within a blind channel, around barchan sediment waves or on gravel ridges and

occur as isolated or, more commonly, clustered examples (Wheeler, Beck, et al., 2005). They can be divided into 4 different areas based on their geographic distribution: the upslope area, the northern area, the downslope area and the midslope area. The Moira Mounds within the downslope area, where the Piddington Mound resides, are concentrated within part of the Arwen Channel (Murphy and Wheeler, 2017; Van Rooij, 2004). This area has been described as favourable for CWC mound development with current speeds of approximately 40 cm s⁻¹ (Lim, 2017). The surrounding seabed is dominated by dropstones while the Piddington Mound itself is dominated by *Lophelia pertusa* and *Madrepora oculata* colonies. It has four distinct facies (live coral framework, dead coral framework, coral rubble and hemipelagic sediment with dropstones) occurring in a ring-like distribution around the mound summit (Lim et al., 2017).

<Insert Figure 1>

2.2 Video data

Two ROV-video datasets were collected for this research. The first video dataset (referred to from here on as “T1”) was collected during the *VENTuRE* survey (2011) on board *RV Celtic Explorer* with the *Holland 1* ROV (cruise number CE11009: Wheeler and shipboard party, 2011). The second video dataset (referred to from here on as “T4”) was collected during the *QuERCi* survey (2015) on board *RV Celtic Explorer* with the *Holland 1* ROV (cruise number CE15009: Wheeler and shipboard party, 2015). Both research cruises collected video data over the Piddington Mound using a downward-facing HD camera mounted on the bottom of the ROV. Positioning and navigation for the ROV during dives were achieved using a Sonardyne Ranger 2 USBL (ultra-short baseline positioning system) corrected by RDI Workhouse doppler velocity logger. The ROV altimeter recorded and logged the height of the ROV (and therefore camera) above the seabed. The ROV recorded downward-facing HD video during a series of

transects covering the entire surface of the Piddington Mound. To maintain a clear image of the mound surface, the ROV was flown <2 m above the mound surface at a survey speed of <2 knots. Several lights were attached to the ROV to achieve homogenous lighting across the camera field of view.

The T1 ROV-video dataset was converted into a video mosaic (Lim, 2017; Lim et al., 2017) using the IFREMER in-house software *Matisse* where the images were extracted from the raw video data at a rate of 1 per second. Poor quality video data (from imagery flown at over 2 m above the seabed, or collected in poor water quality or with poor navigation) were excluded from the image extraction process. To lower ROV trajectory noise, all the USBL navigation data were filtered using a sliding median filtering and 2nd order polynomial model fit. The extracted images and filtered navigation were then synced so each image had an approximate position, which is later refined by the mosaicking process. At this point, features in the extracted images were both detected and matched using a SIFT (Scale Invariant Feature Transform) Algorithm (Lowe, 1999). Image matching and USBL navigation were merged to give an accurate global position, correct scaling and sufficient local overlapping through a cost function minimisation. This method is similar to Ferrer et al. (2007) except cost function weights are affected according to image and navigation data standard deviations so re-projection errors are minimized in the mosaicking plane rather than the image plane. After the image positions are refined, the mosaic can be drawn incorporating seaming and blending techniques developed by Burt and Adelson (1983) and Kwatra et al. (2003). The resulting video mosaic is shown in Figure 2.

<Insert Figure 2>

The georeferenced T1 video mosaic was imported to ArcMap where a fishnet made up of 0.25 m² cells was overlaid on the Piddington Mound mosaic. A manual classification was carried out on the mosaic using the following classifiers: “hemipelagic sediment with dropstones”, “coral rubble”, “hemipelagic sediment”, “dead coral framework” and “live coral framework” (see Fig. 2). The classified fishnet was saved as a shapefile and plotted in ArcMap (Fig. 3).

<Insert Figure 3 >

2.3 Image sampling analysis

To determine the minimum amount of imagery (photographic or still-video) needed from the Piddington Mound to accurately characterise the diversity of surface facies present, sample size estimation (specific to multinomial proportions) was carried out according to Thompson (1987). While other sample size estimation techniques exist (e.g. Angers, 1974), this particular technique is chosen for its robustness and accuracy even in worst case scenarios i.e. when the population proportions (in this case facies proportions) are all equal. The classified cells from the Piddington Mound describe a multinomial distribution with 6 different classes: “hemipelagic sediment with dropstones”, “coral rubble”, “hemipelagic sediment”, “dead coral framework”, “live coral framework” and “no data” (where there is a data gap as a result of data quality being too low to mosaic). To do this, the confidence interval accuracy was defined by selecting an alpha level (α), which represents the significance level at which the confidence level is calculated (e.g. an alpha level of 0.05 gives a confidence level of 95%) and margin of error (d). This ensured the probability that population proportions (facies proportions) across the whole mound surface were covered by the confidence interval. Thompson (1987) provides a table showing the minimum sample size required once these values are defined (see Table 1). For this study, a confidence interval of 95% was defined (i.e. α of 0.05) with a margin of error

(d) of 0.05 allowing a sample size, X (n if $d=0.05$), to be determined (see Table 1). Note, both smaller values of α and smaller margins of error (d) would require larger sample sizes (X) and this method does not take into account spatial autocorrelation. This does not appear to be an issue as all results occur within the 95% confidence interval regardless.

<Insert Table 1>

To determine the best method for collecting images of the mound surface to most effectively capture mound heterogeneity, a series of potential survey designs were performed for the Piddington Mound in ArcMap and saved as *.shp files (Fig. 4). These are used as a guide for a hypothetical drop camera system or ROV to acquire downward-facing stills or live video from which stills can be extracted. The survey designs include the following: a) SD1 - random points; b) SD2 - south to north transect; c) SD3 - east to west transect; d) SD4 - northwest-southeast diagonal transect; e) SD5 - 2 lines; f) SD6 - 3 straight, parallel line grid; g) SD7 - 3 summit-crossing lines; h) SD8 - horizontal grid; i) SD6 - spiral (circling from the mound base to the mound summit) and; j) SD7 - actual survey example (taken from ROV reconnaissance dive navigation over the Piddington Mound). Using the “create random points” tool in ArcMap, X number of random points were generated across the surface of the Piddington Mound (SD1). To collect random points from anywhere on the mound surface, the full mound surface must therefore be imaged thus, SD1 represents the scenario of having full-mound video mosaic coverage. Then, to represent each of the other scenarios, X number of random points were generated across the fishnet but restricted to the lines defining each survey design *.shp file (SD2 to SD10: Figure 4). The proportion of cells of each class for each survey design was calculated. The total number of 0.25 m^2 cells in the fishnet from each class were also counted and the proportion of these cells calculated. This acts as the real-life control against which

results from each survey design can be compared. The results were graphed and the number of “no data” values recorded within each survey design are used to generate proportional error bars for each individual class.

<Insert Figure 4>

2.4 Temporal variability analysis

A repeat survey of the Piddington Mound was undertaken four years after T1 and termed T4. The T4 survey comprises parallel north-south video lines covering the whole mound. In line with the image sampling analysis methodology established herein, a minimum of number of images (X) were extracted from the T4 ROV video dataset with an equal number of images extracted from each video line to ensure a homogenous spread of images across the Piddington Mound surface. The video lines covering 100% of the mound, offer a comparison of the T1 Piddington Mound mosaic after a 4-year interval and in survey design is comparable to “SD1 - random points”.

Each extracted image was manually inspected. A cell (25 cm x 25 cm) is overlaid around the area of the photo where the laser scales pointed (central field of view) and a manual classification was applied using the same classifiers as the T1 ROV video data set: “hemipelagic sediment with dropstones”, “coral rubble”, “hemipelagic sediment”, “dead coral framework” and “live coral framework”. The total number of cells from each class were counted and their proportion determined.

3 Results

3.1 Seabed classification

Figure 3 shows the classified fishnet over the Piddington Mound. 6 classes exist: “hemipelagic sediment with dropstones”, “coral rubble”, “hemipelagic sediment”, “dead coral framework”, “live coral framework” and “no data”. These classes are described in Table 2. There are 5637 cells across the surface of Piddington Mound with the most common being “coral rubble” ($36.1 \pm 3.13\%$) and “dead coral framework” ($31.6 \pm 2.74\%$). The least common cell-types are “hemipelagic sediment” ($1.1 \pm 0.09\%$) and “hemipelagic sediment with dropstones” ($6.7 \pm 0.58\%$). The “live coral framework” cells cover $16.3 \pm 1.42\%$ of the mound surface. While the “coral rubble” cell-type is found across the mound surface, it is typically concentrated around the mound perimeter and on the mound summit. The “live coral framework” cells occur most frequently towards the north of the mound. The “dead coral framework” can be found on the mound flanks. For the remainder of the text, the proportions of all observed cell-types on the Piddington Mound are referred to as the *control proportion*.

<Insert Table 2>

3.2 Image sampling analysis

Sample size estimation according to Thompson (1987), reveals a sample size, X (n if $d=0.05$), of 510 as a minimum sample size to reliably replicate, with a confidence level of 95%, the proportion of facies in the total of 5637 classified cells in the 0.25 m^2 fishnet overlay on the T1 Piddington Mound video-mosaic. The number of categories in our sample size is 6 which is greater than the required minimum of 3.

Figure 5 shows the results of the image sampling analysis for each survey design (more information can be found in the supplementary data supplied with the online version) as facies sampling curves. Survey design “SD1 - random points” (Fig. 5A) represents maximum video coverage and thus the ability to drop 510 random points anywhere across the Piddington Mound surface. This survey design resulted in a 5.9% total difference in facies from the control, namely of the actual proportion of all cells covering the Piddington Mound. The maximum difference in an individual class is 2.9% (“dead coral framework”) with an average class difference of 1.2%.

<Insert Figure 5 >

Survey design “SD2 - south to north transect” (Fig. 5B) represents 510 random image sampling points anywhere along a straight, individual ROV video line from the southern end to the northern end of the Piddington Mound. The line is 50 m in length taking approx. 3.2 minutes for an ROV to complete at 0.5 knots. This survey design resulted in a total of 22.5% difference to that of the actual proportion of all cells covering the Piddington Mound. The maximum difference in an individual class is 6.3% (“dead coral framework”) with an average class difference of 4.1%.

Survey design “SD3 - east to west transect” (Fig. 5C) represents 510 random image sampling points anywhere along a straight, individual ROV video line from the eastern edge to the western edge of the Piddington Mound. The line is 40 m in length taking approx. 2.5 minutes for an ROV to complete at 0.5 knots. This survey design resulted in a total of 11.8% difference to that of the actual proportion of all cells covering the Piddington Mound. The maximum difference in an individual class is 5.8% (“hemipelagic sediment with dropstones”) with an average class difference of 1.7%.

277 Survey design “SD4 - northwest-southeast diagonal transect” (Fig. 5D) represents 510 random
278 image sampling points anywhere along a straight, individual ROV video line from the north-
279 western edge to the south-eastern edge of the Piddington Mound. The line is 40 m in length
280 taking approx. 2.5 minutes for an ROV to complete at 0.5 knots. This survey design resulted
281 in a total of 22.4% difference to that of the actual proportion of all cells covering the Piddington
282 Mound. The maximum difference in an individual class is 7.6% (“live coral framework”) with
283 an average class difference of 2.9%.

284 Survey design “SD5 - 2 lines” (Fig. 5E) represents 510 random image sampling points
285 anywhere along 2 straight ROV video lines (SD2 + SD3) intersecting each other at the summit
286 of the Piddington Mound. This survey covers a line length of 90 m taking approx. 5.8 minutes
287 for an ROV to complete at 0.5 knots. This survey design resulted in a total of 12.4% difference
288 to that of the actual proportion of all cells covering the Piddington Mound. The maximum
289 difference in an individual class is 4.7% (“hemipelagic sediment with dropstones”) with an
290 average class difference of 2.0%.

291 Survey design “SD6 - 3 straight, parallel line grid” (Fig. 5F) represents 510 random image
292 sampling points anywhere along 3 straight, parallel ROV video lines traversing the Piddington
293 Mound in a north-south orientation. This survey covers a line length of 130 m taking approx.
294 8.4 minutes for an ROV to complete at 0.5 knots. This survey design resulted in a total of
295 22.9% difference to that of the actual proportion of all cells covering the Piddington Mound.
296 The maximum difference in an individual class is 9.7% (“hemipelagic sediment with
297 dropstones”) with an average class difference of 3.8%.

298 Survey design “SD7 - 3 summit-crossing lines” (Fig. 5G) represents 510 random image
299 sampling points anywhere along 3 straight, parallel ROV video lines traversing the Piddington
300 Mound (SD2 + SD3 + SD4). This survey covers a line length of 130 m taking approx. 8.4

301 minutes for an ROV to complete at 0.5 knots. This survey design resulted in a total of 11.1%
302 difference to that of the actual proportion of all cells covering the Piddington Mound. The
303 maximum difference in an individual class is 3.4% (“dead coral framework”) with an average
304 class difference of 1.8%.

305 Survey design “SD8 - horizontal grid” (Fig. 5H) represents 510 random image sampling points
306 anywhere along an east-west grid of ROV video lines covering the Piddington Mound. This
307 survey covers a line length of 320 m taking approx. 20.7 minutes for an ROV to complete at
308 0.5 knots. This survey design resulted in a total of 5.8% difference to that of the actual
309 proportion of all cells covering the Piddington Mound. The maximum difference in an
310 individual class is 2.9% (“coral rubble”) with an average class difference of 1.1%. It is also
311 worth noting that there was 0% cell difference in 3 classes.

312 Survey design “SD9 - spiral” (Fig. 5I) represents 510 random image sampling points anywhere
313 along a spiral or conical ROV video line circling from the mound perimeter to the mound flank
314 to the mound summit. This survey covers a line length of 240 m taking approx. 15.5 minutes
315 for an ROV to complete at 0.5 knots. This survey design resulted in a total of 13.4% difference
316 to that of the actual proportion of all cells covering the Piddington Mound. The maximum
317 difference in an individual class is 4.1% (“dead coral framework”) with an average class
318 difference of 2.2%.

319 Survey design “SD10 - actual survey example” (Fig. 5J) represents 510 random image
320 sampling points along an actual ROV reconnaissance dive video line over the Piddington
321 Mound. This survey covers a line length of 1283 m taking 83 minutes for the ROV to complete
322 at 0.5 knots. This survey design resulted in a total of 17.7% difference to that of the actual
323 proportion of all cells covering the Piddington Mound. The maximum difference in an

individual class is 6.7% (“hemipelagic sediment with dropstones”) with an average class difference of 3.4%.

3.3 Temporal variability analysis

Figure 6 and Table 3 show the results of the temporal variability of the Piddington Mound surface data based on a comparison to class determinations in the T1 and T4 video survey data. The minimum number of random samples needed to characterise the mound with a 0.95 probability of being within 0.05 of the class proportions is 510. Here, 622 images are used which marginally increases accuracy above 95% confidence. The most common T4 cell-types are “coral rubble” (43.6%) and “dead coral framework” (37.3%). The “live coral framework” cell-type occurs 16.7% of the time. The least common cell types are “hemipelagic sediment” (1%) and “hemipelagic sediment with dropstones” (1.4%). An important limiting factor of this result is that the error bars developed (Fig. 6 and Table 3) must be considered when comparing the T1 and T4.

<Insert Figure 6>

<Insert Table 3>

4 Discussion

4.1 Seabed imagery for cold water coral mound characterisation

Numerous CWC mounds have been studied incorporating video observations from ROV-mounted camera systems in various different ways: oblique-angled, forward-facing camera

(Foubert et al., 2005), downward-facing camera (Huvenne et al., 2016), both downward-facing and oblique-angled, forward-facing cameras (Dolan et al., 2008; Guinan et al., 2009) and up to 3 cameras (Savini et al., 2014; Vertino et al., 2010). In this study, we focus only on downward facing cameras and we question the effect of the amount of imagery used and the survey design by which it was collected which often varies from study to study. Here, the amount and survey design of seabed imagery acquisition is examined to put forward a survey-feasible methodology for characterising the surface of CWC mounds.

4.1.1 How much seabed imagery is needed to characterise the Piddington Mound?

In the deep sea, sampling and surveying opportunities are limited due to the availability, financial expense and weather-dependency of ship-time on research vessels. As a result, deep-marine data collection is strictly prioritised by urgency of data needs, quite often to meet the needs of funding sources. As such, studies have used “single-pass” (individual line, typically straight) video lines across the surface of CWC mounds to ground truth their surface (e.g. Foubert et al., 2005; Huvenne et al., 2016). While this offers the opportunity to increase the geographical range of the study, it decreases the potential confidence and representativeness of the study. This leads to the question, how much imagery is actually needed to create a reliable representation of the surface of a CWC mound?

Based on the seabed classification (Figure 3), the mound surface sediment facies proportion of 0.25 cm² cell-types on the Piddington Mound are known. Our sample size estimation shows that 510 is the minimum number of 0.25 cm² images needed to accurately determine the proportion of identified classes on the Piddington Mound. Survey design “SD1 - random points” represents the ability to drop 510 random points anywhere on the Piddington Mound, thus utilizing the same video coverage as the T1 ROV video data set (full mound coverage).

Therefore, it can be used to assess and ground-truth the accuracy of the determined sample size. A comparison of the control proportion (Figure 5; All T1) with survey design “SD1 - random points” (Figure 5) shows that this estimation is within 5.9% of the correct proportion of cell-types observed on the Piddington Mound, in line with the aimed probability (at least 0.95 that all estimates are within 0.05 of the multinomial proportions) of this dataset and gives the most reliable representation of the mound surface of all the survey designs tested. The “SD1 - random points” survey could be accomplished by sub-sampling a video-mosaic (100% mound coverage) which, perhaps not surprisingly, is the most robust approach to characterising the mound surface. This could alternatively be accomplished by the use a yo-yo drop camera.

Vertino et al. (2010) examine CWC meso- and macro-scale habitats at the Santa Maria di Leuca Coral Province, a clear example of the utilisation of dense ROV video coverage on CWC mounds and associated habitats to produce detailed studies. The detail revealed by studies with dense video coverage per CWC mound raises the question: are the spatial representation of “single-pass” video line surveys across CWC mounds enough? And conversely, with strict research cruise schedules, at what point does video coverage become *excessive*?

Single-pass ROV video lines across CWC mounds are common (i.e. Dolan et al., 2008; Lim, 2017). As such, 3 different straight line survey designs are tested here (“SD2 - south to north”, “SD3 - east to west” and “SD4 - northwest-southeast diagonal transect”) (Fig. 4 and 5). With an average of 18.9% total difference in cell-type proportions from the control proportion, single-pass surveys appear to yield the least representative results. This is expected given the reduced spatial representation of such survey designs. Two of these survey designs (“SD2 - south to north” and “SD4 - northwest-southeast diagonal transect”) produce a total difference of 22.5% and 22.4% in cell-type proportion from the control proportion, while “SD3 - east to west” produces a total difference of 11.8%. The ring-like cell-type clustering that exists on the Piddington Mound (Lim et al., 2017) appears to have an influence on this result as the course

of the east to west line happens to cover an area with similar proportions to the control proportion. This is evidenced by approximately 50% of the total difference of this survey design resulting from 1 individual facies.

“SD5 - 2 lines” demonstrates the effect of adding a second line to one of these single-pass ROV video lines, in this case SD2 and SD3. This shows an increase in accuracy of 6.5% from single pass surveys (18.9%) to the 2 line survey (12.4%). “SD7 - 3 summit crossing lines” demonstrates the effect of adding a third line (SD2 + SD3 + SD4) to these 2 lines. This shows an increase in accuracy of 1.3% from the 2 line (12.4%) (SD 2 + SD3) survey to the 3 line (11.1%) (SD2 + SD3 + SD4) survey. As such, doubling the number of lines from 1 to 2 increased the accuracy by 6.5% while adding the third line increased the accuracy by just 1.3% while adding 2.6 minutes of extra survey time. Interestingly, a comparison of these 3 summit-crossing lines with 3 lines collected in a grid (SD6), both surveys the same length and time (130 m; 8.4 minutes), highlights the effect of survey design on results where “SD6 - 3 line grid” produced notably less-accurate results (22.9% total difference in facies proportions from the control proportion).

Another common survey design is following the geomorphology of the CWC mound (i.e. Guinan et al., 2009) or some other known characteristic. In the case of the Piddington Mound, survey design “SD9 - spiral” (Fig. 4 and 5) follows both the bathymetry and ring-like growth already observed on the Piddington Mound (Lim et al., 2017), circling through the mound perimeter, flank and summit. This cone-like survey design yields a 13.4% total cell-type proportion difference from the control proportion. The accuracy of this result is probably due to the influence of prior knowledge on survey design.

Survey design “SD10 - actual survey” defines the navigation path of an ROV on a reconnaissance dive over the Piddington Mound when it was first discovered and initially

417 investigated (Wheeler and shipboard party, 2011) (Fig. 4 and 5). This survey design yields a
418 17.7% total cell-type proportion difference from the control proportion. It represents a real-life
419 example of survey design without the influence of prior knowledge or mapping of the CWC
420 mound. This survey design (or lack of) resulted in relatively a large (7.6%) over-estimation of
421 “live coral framework” cell-types. This sampling bias may be typical of reconnaissance video
422 investigations when discovering new seabed features as scientists may preferentially
423 concentrate the cameras on the live proportion of the feature that is of more interest to them.
424 Another short-coming of this survey design, and probably a result of the same sampling bias,
425 is that 2 entire classes were not seen in the video observation (“hemipelagic sediment with
426 dropstones” and “hemipelagic sediment”). Interestingly, this survey covered a line length of
427 1283 m (83 survey minutes), over 1000 m more than the aforementioned surveys designs. As
428 such, this once again highlights the importance of survey design over line length.

429 Probably the most well-known survey design, but apparently least-applied in the case of CWC
430 mounds is survey design “SD8 - horizontal grid” (Fig. 4 and 5). In this example, the grid is
431 made up of a series of mound-traversing lines spaced approximately 5 m apart where the end
432 of each line is connected to the start of the next line. This survey design yields a 5.8% total
433 cell-type proportion difference from the control proportion, the most representative proportion
434 of the study. An additional positive of this survey design is that it estimated the exact proportion
435 of individual cell-types for 3 classes (“hemipelagic sediment with dropstones”, “hemipelagic
436 sediment” and “live coral framework”). Interestingly, it also yields a similar result to survey
437 design “SD1 - random points” (5.9%) which represents full-mound video coverage. With line
438 spacing of approx. 1 m, it took ~8 hours to collect the full-mound video coverage (Wheeler and
439 shipboard party, 2011). Assuming a survey speed of 0.5 knots to collect survey design “SD8 -
440 horizontal grid” (line length of 320 m), it would take 20.7 minutes to collect this ROV video
441 data, a vast improvement from ~8 hours for the same representation of surface facies

proportions. In addition, this technique appears to be unbiased by the significant clustering found on the Piddington Mound (Lim et al., 2017).

4.2 What is the temporal variability of Piddington Mound and its implication for samples?

The T4 ROV-video dataset was collected over the Piddington Mound 4 years after the T1 survey (2015) covering the entire mound surface with the same downward-facing camera array. To assess mound surface change over this period, 622 random images are classified (a minimum of 510 are needed) according to the image sampling technique established above using the same classifiers. The survey design, similar to the T1 ROV video data set, covers the entire mound surface by a 1 m spaced line grid. Thus, the accuracy of this data is similar to that of survey design “SD1 - random points” (Fig. 5).

The T4 ROV video dataset exhibits a change of 19% of the total mound surface in comparison to the T1 ROV video dataset. This change has taken place over 4 years (2011 - 2015) and is evident at a 25 cm² resolution. The “live coral framework” cell-type remains relatively constant, increasing by only 0.4% over the 4 years (+0.1% per year). A minute increase is expected given the slow growth rates (15 - 30 mm yr⁻¹) observed in *Lophelia* (Gass and Roberts, 2006; Larcom et al., 2014; Orejas et al., 2008). Similarly, Huvenne et al. (2016) show that after ten years, the amount of live coral found on the Darwin Mounds, the only other known example of small-sized CWC mounds in the NE Atlantic, also remains the same. The “normal” proportion of live coral per Darwin Mound is ~45-55%, sizably greater than that found here on the Piddington Mound.

The “hemipelagic sediment” cell-type also remains relatively constant (-0.2% over 4 years) given the minute change and size of the potential error margin (Table 3). This facies is typically found in the lee of “live coral framework” cell-types (Fig. 3) where it is protected from

resuspension by the current (Lim et al., 2017). As such, given the fact that the proportion of “live coral framework” cells have not changed, it seems likely that the proportion of “hemipelagic sediment” cell-type would remain the same.

The “coral rubble” cell-type increased the most (7.5%) at a rate of 1.9% per year, assuming a constant rate of change. Given the dominance of the “coral rubble” cell-type on Piddington Mound in 2011, it is likely to see a change in the proportion of this class. The source of this coral rubble is likely to be as a result of the biological or physical erosion of the “dead coral framework” class (Lim et al., 2017) or on-mound (re)exposure and redistribution through benthic erosion and transport processes.

Interestingly, the proportion of “dead coral framework” cell-type increased by 5.7% (a rate of 1.4% per year). If this class is both contributing to the “coral rubble” class and increasing relative to the T1 “dead coral framework” class, then it can be assumed that it changed by at least 5.7% and at a minimum of 1.4% per year. Given the low growth rate of *Lophelia* mentioned earlier, it is unlikely that the source of the increased “dead coral framework” coverage is entirely from the degradation of the “live coral framework” cell-type. It is therefore suggested that this increase is possibly through “dead coral framework” exhumation by currents removing covering sediment. Although there has been impact of demersal trawling on the seabed in the area (Foubert et al., 2005; Wheeler, Beck, et al., 2005), the Belgica Mound Province is now an SAC (special area of conservation). As such, it is less likely that trawling has impacted the movement of dead coral framework on the mound during the course of the study.

The proportion of the “sediment and dropstone” class decreases the most (-5.3%) at a rate of 1.3% per year. Given the mound-perimeter occurrence of this class and the dominance of the “coral rubble” on the steepest parts of the mound (flanks), it is likely that this decrease is due to burial by coral rubble where the coral rubble (or freshly eroded coral rubble from dead coral

frameworks) roll from the steepened mound flanks to the edges of the mound where the slope decreases and “sediment and dropstone” cell-types are common (Lim et al., 2017).

Based on the results herein and cautiously assuming a linear rate of change of a total mound surface change of 4.8% per year, then in just over 20 years, this suggests the entire Piddington Mound surface will change. Thus, if physical and image (video or photographic) samples are taken 5 years apart on Piddington Mound, a change of 25% (and 50% after 10 years) on the mound surface influences whether or not these samples consistently represent the mounds’ status in the contemporary environment. This, coupled with the heterogeneity observed on the CWC mounds, positioning error margins (e.g. ~2 m with some calibrated USBL systems in deep water) and inconsistencies of repeat video acquisition (Purser, 2015) contests the validity of interpretation from surface samples on similar CWC mounds. It is therefore recommended that data from various survey campaigns should be treated cautiously as they may not represent the “contemporary” environment. As such, we strongly recommend to use samples collected during the same survey to represent the contemporary environment (e.g. samples collected in 2017 to be used only with video coverage from 2017) if possible.

Centimetre-scale, remotely-sensed mapping is becoming more common in the marine environment. As such, observations from video data should be equally as accurate. Oblique camera data acquisition induces positional errors where there is an offset between the field of view of the camera and the positioning beacon (e.g. USBL) thus giving an incorrect position for oblique camera video observation. This error is a function of camera obliqueness, rotation of the camera-mounted platform (e.g. ROV) around its axis, seabed slope and height of camera from seabed and is therefore not constant nor easily reconciled. For relevant example, oblique camera data has been utilized in a temporal study of a CWC mound, offshore Norway, which highlights the inconsistencies of repeat surveys using oblique camera (e.g. viewing the same part of the mound from different angles) (Purser, 2015). As such, we would like to recommend

the use of downward-facing camera for temporal-based studies of CWC habitats (and other dynamic marine habitats) as positioning of the camera is not influenced by rotation of the camera around its axis, the angle at which it views the seabed is always the same (0°) and is not influenced by seabed slope in the same way as oblique camera.

5 Conclusion

This study presents an assessment of video survey design specific to a CWC mound (the Piddington Mound of the Moira Mounds, NE Atlantic) to assess both differences in surface facies proportion and temporal facies proportion. The technique presented is developed with particular consideration for the financial, temporal and sea-state dependant nature of deep sea research to maximise resolution and spatial coverage. Known proportions of CWC-typical facies on the Piddington Mound were used to determine the minimum number of images needed to characterise the surface of similar-sized CWC mounds with the same number of classes using downward-facing camera. This allows for a standardised approach to surveying and studying CWC mounds through video and comparison of mounds in different geographic settings and in time at 25 cm² resolution. A comparison of different common survey designs show that single-pass video are the least-representative and highly-influenced by the heterogeneity, typical of CWC mounds, despite being commonly utilised in research. Following bathymetry or known features on CWC mounds is another common survey design but does not yield the most accurate results. The most representative results were yielded from either fully video mosaicking a mound or using a grid of spaced lines. However, a grid of lines in this case requires 1/16 of the time required for video mosaicking an entire mound while yielding similar results.

The developed technique was applied to the Piddington Mound 4 years later to assess the change in proportions of facies across the mound surface. With a mound surface change of

4.8% per year, the mound surface has changed by almost 20% from 2011 to 2015. The greatest change was in the “coral rubble” class (7.5%) followed by “dead coral framework” and “sediment and dropstone” classes. These classes are affected by strong currents as mobile or exhumed substrates. Similar to other mounds, the proportion of “live coral framework” class remained the same over the 4-year period as anticipated for a sessile slow growing organism. Although assuming a linear rate of change, we suggest that in approx. 20 years, ~100% change in the surface of the Piddington Mound. Thus, samples taken from the mound 5 years apart (with a 25% mound surface change), makes the samples inconsistent and therefore not representative of the contemporary mound status. We also stress that in utilising this technique, the potential error bars must be taken into consideration when comparing between data sets. Finally, we highlight the suitability of downward-facing camera for high-resolution repeat surveys for temporal variability purposed due to the many short-comings of temporal-based, oblique-camera surveys.

6 Acknowledgements

The authors would like to sincerely thank Boris Dorschel for his extremely useful input and proofing of this work, Evan Edinger and another anonymous reviewer for their timely and insightful reviews. We would like to thank the crew and officers of ROV Holland 1 and RV Celtic Explorer for assistance in collecting high resolution, accurately positioned data. Ship time on the RV Celtic Explorer was funded by the Marine Institute under the 2011 and 2015 Ship Time Programme of the National Development Plan. Mohit Tunwal (UCC) is thanked for mathematical proofing.

561 7 References

- 562 Angers, C., 1974. A graphical method to evaluate sample sizes for the multinomial distribution.
 563 Technometrics 16, 469-471, <http://dx.doi.org/10.1080/00401706.1974.10489219>.
- 564 Beyer, A., Schenke, H.W., Klenke, M., Niederjasper, F., 2003. High resolution bathymetry of
 565 the eastern slope of the Porcupine Seabight. Marine Geology 198, 27-54,
 566 [http://dx.doi.org/10.1016/S0025-3227\(03\)00093-8](http://dx.doi.org/10.1016/S0025-3227(03)00093-8).
- 567 Burt, P.J., Adelson, E.H., 1983. A Multiresolution Spline with Application to Image Mosaics.
 568 Acm Transactions on Graphics 2, 217-236, Doi 10.1145/245.247.
- 569 Chitre, M., Shahabudeen, S., Stojanovic, M., 2008. Underwater acoustic communications and
 570 networking: Recent advances and future challenges. Marine Technology Society Journal 42,
 571 103-116, <http://dx.doi.org/10.4031/002533208786861263>.
- 572 Correa, T.B.S., Eberli, G.P., Grasmueck, M., Reed, J.K., Correa, A.M.S., 2012. Genesis and
 573 morphology of cold-water coral ridges in a unidirectional current regime. Marine Geology 326,
 574 14-27, 10.1016/j.margeo.2012.06.008.
- 575 Davies, A.J., Guinotte, J.M., 2011. Global Habitat Suitability for Framework-Forming Cold-
 576 Water Corals. PLoS ONE 6, e18483, 10.1371/journal.pone.0018483.
- 577 Davies, A.J., Wisshak, M., Orr, J.C., Roberts, J.M., 2008. Predicting suitable habitat for the
 578 cold-water coral *Lophelia pertusa* (Scleractinia). Deep-Sea Research I 55, 1048-1062,
 579 <http://dx.doi.org/10.1016/j.dsr.2008.04.010>.
- 580 De Mol, B., Kozachenko, M., Wheeler, A.J., Alvares, H., Henriët, J.-P., Olu-Le Roy, K., 2007.
 581 Thérèse Mound: a case study of coral bank development in the Belgica Mound Province,
 582 Porcupine Seabight. International Journal of Earth Sciences 96, 103-120,
 583 <http://dx.doi.org/10.1007/s00531-005-0496-x>.
- 584 Dolan, M.F.J., Grehan, A.J., Guinan, J.C., Brown, C., 2008. Modelling the local distribution
 585 of cold-water corals in relation to bathymetric variables: Adding spatial context to deep-sea
 586 video data. Deep-Sea Research I 55, 1564-1579, <http://dx.doi.org/10.1016/j.dsr.2008.06.010>.
- 587 Dorschel, B., 2003. Late Quaternary Development of a deep-water Carbonate Mound in the
 588 northeast Atlantic, RCOM-Bremen. University of Bremen, bremen, p. 90.
- 589 Dorschel, B., Wheeler, A.J., Huvenne, V.A.I., de Haas, H., 2009. Cold-water coral mounds in
 590 an erosive environmental setting: TOBI side-scan sonar data and ROV video footage from the
 591 northwest Porcupine Bank, NE Atlantic. Marine Geology 264, 218-229,
 592 10.1016/j.margeo.2009.06.005.
- 593 Douarin, M., Sinclair, D.J., Elliot, M., Henry, L.-A., Long, D., Mitchison, F., Roberts, J.M.,
 594 2014. Changes in fossil assemblage in sediment cores from Mingulay Reef Complex (NE
 595 Atlantic): Implications for coral reef build-up. Deep Sea Research Part II: Topical Studies in
 596 Oceanography 99, 286-296, <http://dx.doi.org/10.1016/j.dsr2.2013.07.022>.

597 Dullo, W.-C., Flögel, S., Rüggeberg, A., 2008. Cold-water coral growth in relation to the
598 hydrography of the Celtic and Nordic European continental margin. *Marine Ecology Progress*
599 *Series* 371, 165-176, 10.3354/meps07623.

600 Eisele, M., Hebbeln, D., Wienberg, C., 2008. Growth history of a cold-water coral covered
601 carbonate mound - Galway Mound, Porcupine Seabight, NE-Atlantic. *Marine Geology* 253,
602 160-169, 10.1016/j.margeo.2008.05.006.

603 Ferrer, J., Elibol, A., Delaunoy, O., Gracias, N., Garcia, R., 2007. Large-area photo-mosaics
604 using global alignment and navigation data, MTS/IEEE OCEANS Conference, Vancouver,
605 Canada, pp. 1-9, <http://dx.doi.org/10.1109/OCEANS.2007.4449367>.

606 Foubert, A.T.G., Beck, T., Wheeler, A.J., Opderbecke, J., Grehan, A., Klages, M., Thiede, J.,
607 Henriët, J.-P., Polarstern ARK-XIX/3a shipboard party, 2005. New view of the Belgica
608 Mounds, Porcupine Seabight, NE Atlantic: preliminary results from the Polarstern ARK-
609 XIX/3a ROV cruise, in: Freiwald, A., Roberts, J.M. (Eds.), *Deep-water corals and Ecosystems*,
610 . Springer-Verlag, Berlin Heidelberg, pp. 403-415.

611 Freiwald, A., 2002. Reef-Forming Cold-Water Corals, in: Wefer, G., Billett, D.S.M., Hebbeln,
612 D., Jørgensen, B.B., van Weering, T.C.E. (Eds.), *Ocean Margin Systems*, Hanse Conference
613 on Ocean Margin Systems (2000: Delmenhorst, Germany) ed. Springer, Berlin Heidelberg
614 New York, pp. 365-385, http://dx.doi.org/10.1007/978-3-662-05127-6_23.

615 Freiwald, A., Fosså, J.H., Grehan, A., Koslow, T., Roberts, J.M., 2004. Cold-water Coral
616 Reefs, NEP-WCMC, Cambridge, UK, p. 88, <http://hdl.handle.net/20.500.11822/8727>.

617 Freiwald, A., Wilson, J.B., 1998. Taphonomy of modern, deep, cold-temperate water coral
618 reefs. *Historical Biology* 13, 37-52, <http://dx.doi.org/10.1080/08912969809386571>.

619 Gass, S.E., Roberts, J.M., 2006. The occurrence of the cold-water coral *Lophelia pertusa*
620 (Scleractinia) on oil and gas platforms in the North Sea: Colony growth, recruitment and
621 environmental controls on distribution. *Marine Pollution Bulletin* 52, 549-559,
622 <http://dx.doi.org/10.1016/j.marpolbul.2005.10.002>.

623 Guinan, J., Grehan, A.J., Dolan, M.F.J., Brown, C., 2009. Quantifying relationships between
624 video observations of cold-water coral cover and seafloor features in Rockall Trough, west of
625 Ireland. *Marine Ecology Progress Series* 375, 125-138, 10.3354/meps07739.

626 Henriët, J.P., Hamoumi, N., Da Silva, A.C., Foubert, A., Lauridsen, B.W., Rüggeberg, A., Van
627 Rooij, D., 2014. Carbonate mounds: From paradox to World Heritage. *Marine Geology* 352,
628 89-110, <http://dx.doi.org/10.1016/j.margeo.2014.01.008>.

629 Huvenne, V.A., Tyler, P.A., Masson, D.G., Fisher, E.H., Hauton, C., Huhnerbach, V., Le Bas,
630 T.P., Wolff, G.A., 2011. A picture on the wall: innovative mapping reveals cold-water coral
631 refuge in submarine canyon. *PLoS ONE* 6, e28755, 10.1371/journal.pone.0028755.

632 Huvenne, V.A.I., Bett, B.J., Masson, D.G., Le Bas, T.P., Wheeler, A.J., 2016. Effectiveness of
633 a deep-sea cold-water coral Marine Protected Area, following eight years of fisheries closure.
634 *Biological Conservation* 200, 60-69, 10.1016/j.biocon.2016.05.030.

635 Huvenne, V.A.I., Beyer, A., de Haas, H., Dekindt, K., Henriët, J.-P., Kozachenko, M., Olu-Le
636 Roy, K., Wheeler, A.J., participants, T.P.c., participants, C.c., 2005. The seabed appearance of

different coral bank provinces in the Porcupine Seabight, NE Atlantic: results from sidescan sonar and ROV seabed mapping, in: Freiwald, A., Roberts, J.M. (Eds.), Cold-water Corals and Ecosystems. Springer-Verlag, Berlin Heidelberg, pp. 535-569, http://dx.doi.org/10.1007/3-540-27673-4_27.

Kinsey, J.C., Eustice, R.M., Whitcomb, L.L., 2006. A survey of underwater vehicle navigation: Recent advances and new challenges, IFAC Conference of Manoeuvring and Control of Marine Craft.

Kwatra, V., Schödl, A., Essa, I., Turk, G., Bobick, A., 2003. Graphcut textures: image and video synthesis using graph cuts, ACM Transactions on Graphics (TOG). ACM, pp. 277-286, <http://dx.doi.org/10.1145/882262.882264>.

Larcom, E.A., McKean, D.L., Brooks, J.M., Fisher, C.R., 2014. Growth rates, densities, and distribution of *Lophelia pertusa* on artificial structures in the Gulf of Mexico. Deep-Sea Research Part I-Oceanographic Research Papers 85, 101-109, 10.1016/j.dsr.2013.12.005.

Lavaleye, M., Duineveld, G., Lundälv, T., White, M., Guihen, D., Kiriakoulakis, K., Wolff, G.A., 2009. Cold-Water Corals on the Tisler Reef-preliminary observations on the dynamic reef environment. Oceanography 22, 76-84, <http://dx.doi.org/10.5670/oceanog.2009.08>.

Lim, A., 2017. Spatio-temporal patterns and controls on cold-water coral reef development: the Moira Mounds, Porcupine Seabight, NE Atlantic, School of Biological, Earth and Environmental Sciences. University College Cork, Cork Open Research Archive, p. 221, <http://hdl.handle.net/10468/4031>.

Lim, A., Wheeler, A.J., Arnaubec, A., 2017. High-resolution facies zonation within a cold-water coral mound: The case of the Piddington Mound, Porcupine Seabight, NE Atlantic. Marine Geology 390, 120-130, <https://doi.org/10.1016/j.margeo.2017.06.009>.

Lowe, D.G., 1999. Object recognition from local scale-invariant features, Computer vision, 1999. The proceedings of the seventh IEEE international conference on Computer Vision. Ieee, pp. 1150-1157, <http://dx.doi.org/10.1109/ICCV.1999.790410>.

Lundälv, T., Fosså, J.H., Buhl Mortensen, P., Jonsson, L.G., White, M., Guihen, D., Unnithan, V., 2008. Development in a trawl-damaged coral habitat (Tisler reef, NE Skagerrak) during four years of trawl protection, 4th International Symposium on Deep-Sea Corals, Wellington, New Zealand, December 2008.

Mangini, A., Lomitschka, M., Eichstädter, R., Frank, N., Vogler, S., Bonani, G.G., Hajdas, I., Pätzold, J., 1998. Coral provides age of deep water. Nature 392, <http://dx.doi.org/10.1038/32804>.

Mortensen, P.B., Hovland, M.T., Fosså, J.H., Furevik, D.M., 2001. Distribution, abundance and size of *Lophelia pertusa* coral reefs in mid-Norway in relation to seabed characteristics. Journal of the Marine Biological Association of the UK Volume 81, Issue 04, Aug 2001, 581-597, <http://dx.doi.org/10.1017/S002531540100426X>.

Murphy, P., Wheeler, A.J., 2017. A GIS-based application of drainage basin analysis and geomorphometry in the submarine environment: The Gollum Canyon System, North-east Atlantic, in: Bartlett, D., Celliers, L. (Eds.), Geoinformatics for Marine and Coastal

677 Management. CRC Press, Taylor & Francis Group, Boca Raton, USA,
678 <http://dx.doi.org/10.1201/9781315181523-4>.

679 Orejas, C., Gori, A., Gili, J.M., 2008. Growth rates of live *Lophelia pertusa* and *Madrepora*
680 *oculata* from the Mediterranean Sea maintained in aquaria. *Coral Reefs* 27, 255-255,
681 10.1007/s00338-007-0350-7.

682 Orejas, C., Gori, A., Rad-Menendez, C., Last, K.S., Davies, A.J., Beveridge, C.M., Sadd, D.,
683 Kiriakoulakis, K., Witte, U., Roberts, J.M., 2016. The effect of flow speed and food size on the
684 capture efficiency and feeding behaviour of the cold-water coral *Lophelia pertusa*. *Journal of*
685 *Experimental Marine Biology and Ecology* 481, 34-40, 10.1016/j.jembe.2016.04.002.

686 Purser, A., 2015. A Time Series Study of *Lophelia pertusa* and Reef Megafauna Responses to
687 Drill Cuttings Exposure on the Norwegian Margin. *PLoS ONE* 10, e0134076,
688 10.1371/journal.pone.0134076.

689 Purser, A., Larsson, A.I., Thomsen, L., van Oevelen, D., 2010. The influence of flow velocity
690 and food concentration on *Lophelia pertusa* (Scleractinia) zooplankton capture rates. *Journal*
691 *of Experimental Marine Biology and Ecology* 395, 55-62, 10.1016/j.jembe.2010.08.013.

692 Raddatz, J., Rüggeberg, A., Liebetrau, V., Foubert, A., Hathorne, E.C., Fietzke, J., Eisenhauer,
693 A., Dullo, W.-C., 2014. Environmental boundary conditions of cold-water coral mound growth
694 over the last 3 million years in the Porcupine Seabight, Northeast Atlantic. *Deep Sea Research*
695 *Part II: Topical Studies in Oceanography* 99, 227-236,
696 <http://dx.doi.org/10.1016/j.dsr2.2013.06.009>.

697 Robert, K., Huvenne, V.A.I., Georgiopoulou, A., Jones, D.O.B., Marsh, L., D. O. Carter, G.,
698 Chaumillon, L., 2017. New approaches to high-resolution mapping of marine vertical
699 structures. *Scientific Reports* 7, 9005, 10.1038/s41598-017-09382-z.

700 Robert, K., Jones, D.O.B., Roberts, J.M., Huvenne, V.A.I., 2016. Improving predictive
701 mapping of deep-water habitats: Considering multiple model outputs and ensemble techniques.
702 *Deep Sea Research Part I: Oceanographic Research Papers* 113, 80-89,
703 <http://dx.doi.org/10.1016/j.dsr.2016.04.008>.

704 Roberts, J.M., Long, D., Wilson, J.B., Mortensen, P.B., Gage, J.D., 2003. The cold-water coral
705 *Lophelia pertusa* (Scleractinia) and enigmatic seabed mounds along the north-east Atlantic
706 margin: are they related? *Marine Pollution Bulletin* 46, 7-20, [http://dx.doi.org/10.1016/S0025-](http://dx.doi.org/10.1016/S0025-326X(02)00259-X)
707 [326X\(02\)00259-X](http://dx.doi.org/10.1016/S0025-326X(02)00259-X).

708 Roberts, J.M., Wheeler, A.J., Cairns, S., Freiwald, A., 2009. Cold-water corals: the biology
709 and geology of deep-sea coral habitats. Cambridge University Press,
710 <http://dx.doi.org/10.1017/CBO9780511581588.003>.

711 Roberts, J.M., Wheeler, A.J., Freiwald, A., 2006. Reefs of the Deep: The Biology and Geology
712 of Cold-Water Coral Ecosystems. *Science* 312, 543-547,
713 <http://dx.doi.org/10.1126/science.1119861>.

714 Rüggeberg, A., Dullo, W.-C., Dorschel, B., Hebbeln, D., 2007. Environmental changes and
715 growth history of a cold-water carbonate mound (Propeller Mound, Porcupine Seabight).
716 *International Journal of Earth Sciences* 96, 57-72.

717 Savini, A., Vertino, A., Marchese, F., Beuck, L., Freiwald, A., 2014. Mapping cold-water coral
718 habitats at different scales within the Northern Ionian Sea (Central Mediterranean): an
719 assessment of coral coverage and associated vulnerability. PLoS ONE 9, e87108,
720 10.1371/journal.pone.0087108.

721 Squires, D.F., 1964. Fossil coral thickets in Wairarapa, New Zealand. Journal Paleontol. 38,
722 904-915.

723 Thompson, S.K., 1987. Sample size for estimating multinomial proportions. The American
724 Statistician 41, 42-46, <http://dx.doi.org/10.2307/2684318>.

725 Van Rooij, D., 2004. An integrated study of Quaternary sedimentary processes on the eastern
726 slope of the Porcupine Seabight, SW of Ireland. Ghent University,
727 <http://dx.doi.org/1854/10815>.

728 Vertino, A., Savini, A., Rosso, A., Di Geronimo, I., Mastrototaro, F., Sanfilippo, R., Gay, G.,
729 Etiope, G., 2010. Benthic habitat characterization and distribution from two representative sites
730 of the deep-water SML Coral Province (Mediterranean). Deep-Sea Research Part II-Topical
731 Studies in Oceanography 57, 380-396, 10.1016/j.dsr2.2009.08.023.

732 Wheeler, A.J., Beck, T., Thiede, J., Klages, M., Grehan, A., Monteys, F.X., Polarstern ARK
733 XIX/3a Shipboard Party, 2005. Deep-water coral mounds on the Porcupine Bank, Irish margin:
734 preliminary results from Polarstern ARK-XIX/3a ROV cruise, in: Freiwald, A., Roberts, J.M.
735 (Eds.), Cold-water corals and Ecosystems. Springer-Verlag, Berlin, pp. 393-402,
736 http://dx.doi.org/10.1007/3-540-27673-4_19.

737 Wheeler, A.J., Beyer, A., Freiwald, A., de Haas, H., Huvenne, V.A.I., Kozachenko, M., Olu-
738 Le Roy, K., Opderbecke, J., 2007. Morphology and environment of cold-water coral carbonate
739 mounds on the NW European margin. International Journal of Earth Sciences 96, 37-56,
740 <http://dx.doi.org/10.1007/s00531-006-0130-6>.

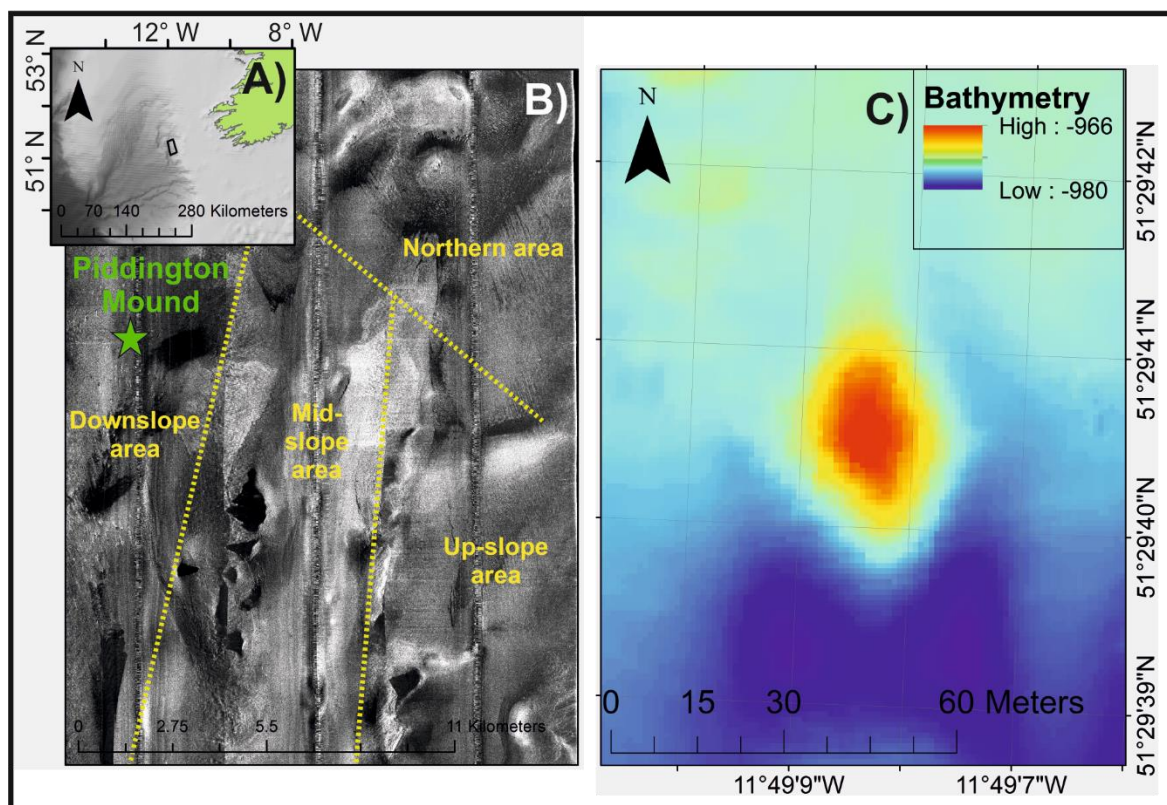
741 Wheeler, A.J., Kozachenko, M., Beyer, A., Foubert, A.T.G., Huvenne, V.A.I., Klages, M.,
742 Masson, D.G., Olu-Le Roy, K., Thiede, J., 2005. Sedimentary processes and carbonate mounds
743 in the Belgica Mound province, Porcupine Seabight, NE Atlantic, in: Freiwald, A., Roberts,
744 J.M. (Eds.), Cold-water Corals and Ecosystems. Springer-Verlag, Berlin Heidelberg, pp. 533-
745 564, http://dx.doi.org/10.1007/3-540-27673-4_28.

746 Wheeler, A.J., Kozachenko, M., Henry, L.A., Foubert, A., de Haas, H., Huvenne, V.A.I.,
747 Masson, D.G., Olu, K., 2011. The Moira Mounds, small cold-water coral banks in the
748 Porcupine Seabight, NE Atlantic: Part A—an early stage growth phase for future coral
749 carbonate mounds? Marine Geology 282, 53-64, 10.1016/j.margeo.2010.08.006.

750 Wheeler, A.J., Kozachenko, M., Masson, D.G., Huvenne, V.A.I., 2008. Influence of benthic
751 sediment transport on cold-water coral bank morphology and growth: the example of the
752 Darwin Mounds, north-east Atlantic. Sedimentology 55, 1875-1887, 10.1111/j.1365-
753 3091.2008.00970.x.

754 Wheeler, A.J., shipboard party, 2011. Vents & Reefs deep-sea ecosystem study of the 45° North
755 MAR hydrothermal vent field and the cold-water coral Moira Mounds, Porcupine Seabight,
756 Cruise report, p. 160.

- Wheeler, A.J., Stadnitskaia, A., 2011. Benthic Deep-Sea Carbonates. Developments in Sedimentology 63, 397-455, <http://dx.doi.org/10.1016/B978-0-444-53000-4.00006-8>.
- White, M., 2007. Benthic dynamics at the carbonate mound regions of the Porcupine Sea Bight continental margin. International Journal of Earth Sciences 96, 1-9, <http://dx.doi.org/10.1007/s00531-006-0099-1>.
- Wienberg, C., Beuck, L., Heidkamp, S., Hebbeln, D., Freiwald, A., Pfannkuche, O., Monteys, F.X., 2008. Franken Mound: facies and biocoenoses on a newly-discovered "carbonate mound" on the western Rockall Bank, NE Atlantic. Facies 54, 1-24, 10.1007/s10347-007-0118-0.
- Wienberg, C., Hebbeln, D., Fink, H.G., Mienis, F., Dorschel, B., Vertino, A., López Correa, M., Freiwald, A., 2009. Scleractinian cold-water corals in the Gulf of Cádiz-first clues about their spatial and temporal distribution. Deep Sea Research Part I 56, 1873-1893, doi:10.1016/j.dsr.2009.05.016.
- Wilson, J.B., 1979. "Patch" development of the deep-water coral *Lophelia pertusa* (L.) on the Rockall bank. Journal of the Marine Biological Association of the United Kingdom 59, 165-177, <http://dx.doi.org/10.1017/S0025315400046257>.



786 *Figure 1 Location map of study area*

787 A) Location of Belgica Mound Province (BMP) Special Area of Conservation (SAC) (black
 788 box), offshore SW Ireland; B) 30 kHz TOBI side scan sonar imagery of the BMP SAC with
 789 areas defined by Wheeler et al., (2011) in yellow and location of Piddington Mound indicated
 790 by green star; C) Piddington Mound bathymetry (meters).

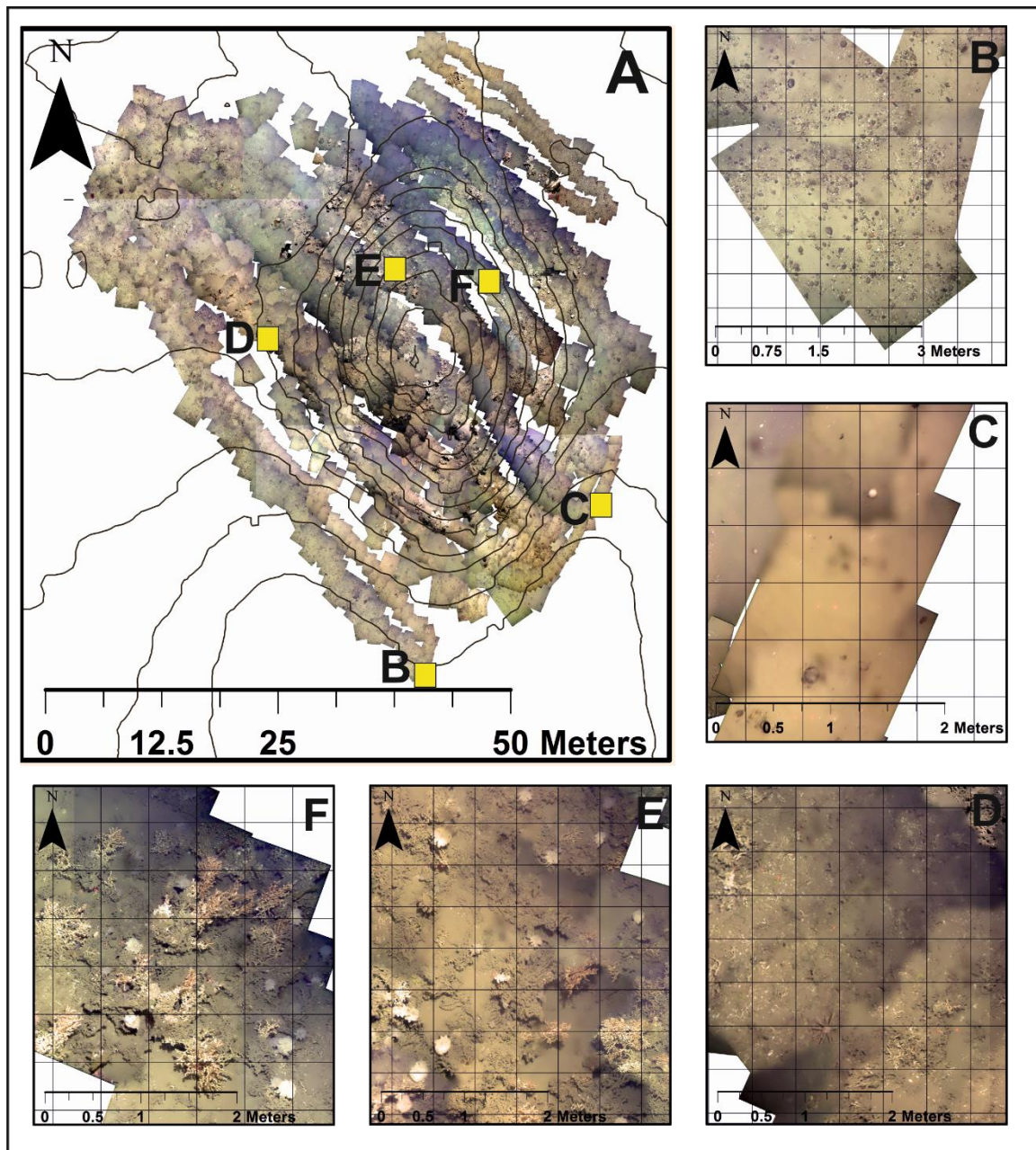


Figure 2 Map of the Piddington Mound video mosaic and examples of classes: A) mosaicked area with 1 m contours superimposed, B) example of the “hemipelagic sediment with dropstones” class, C) example of the “hemipelagic sediment” class, D) example of the “coral rubble” class, E) example of the “dead coral framework” class, and F) example of the “live coral framework” class.

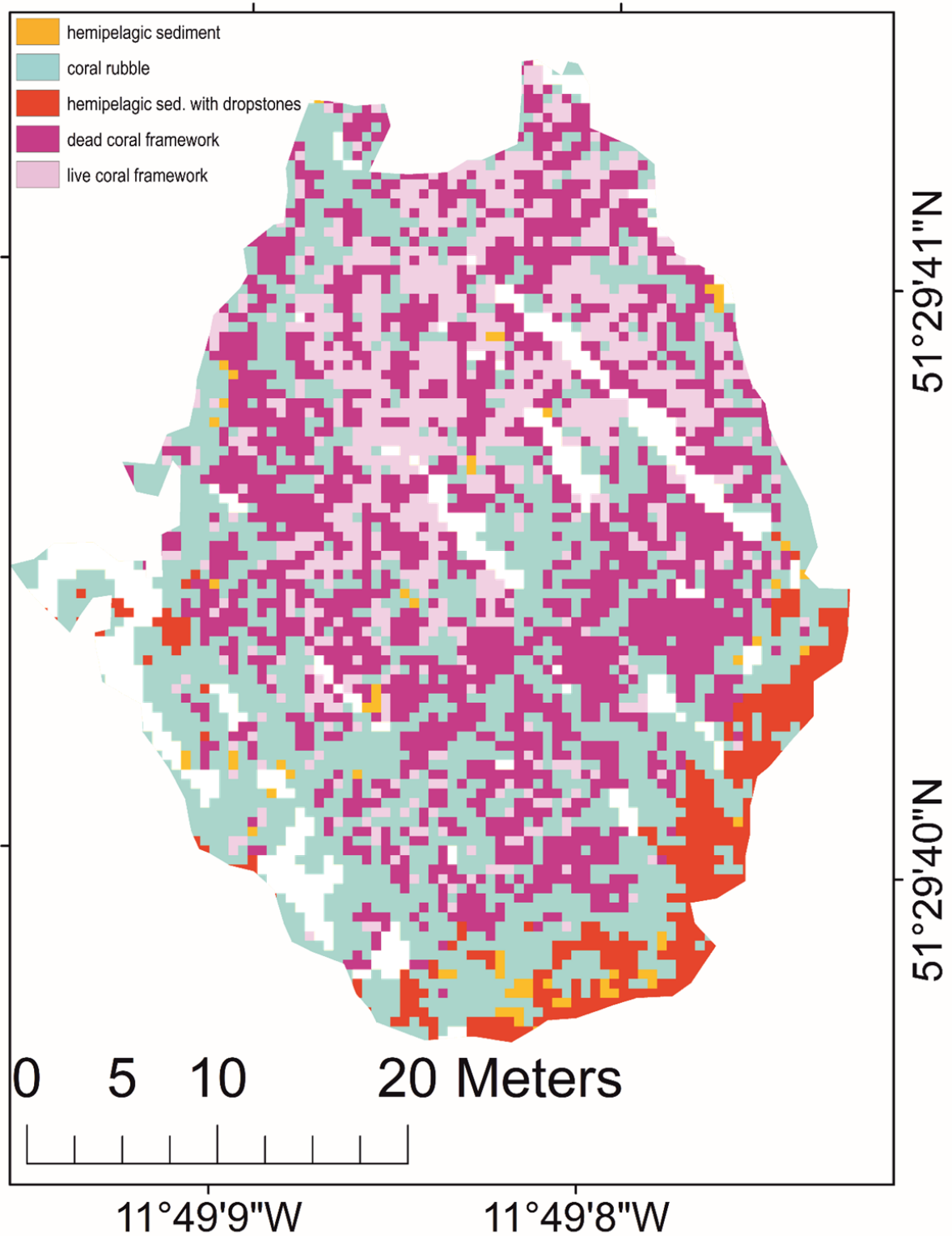


Figure 3 Classified mosaic

Blue= coral rubble cells; red=sediment and dropstone cells; orange= hemipelagic sediment cells; magenta=dead coral framework cells; and pink=live coral framework cells.

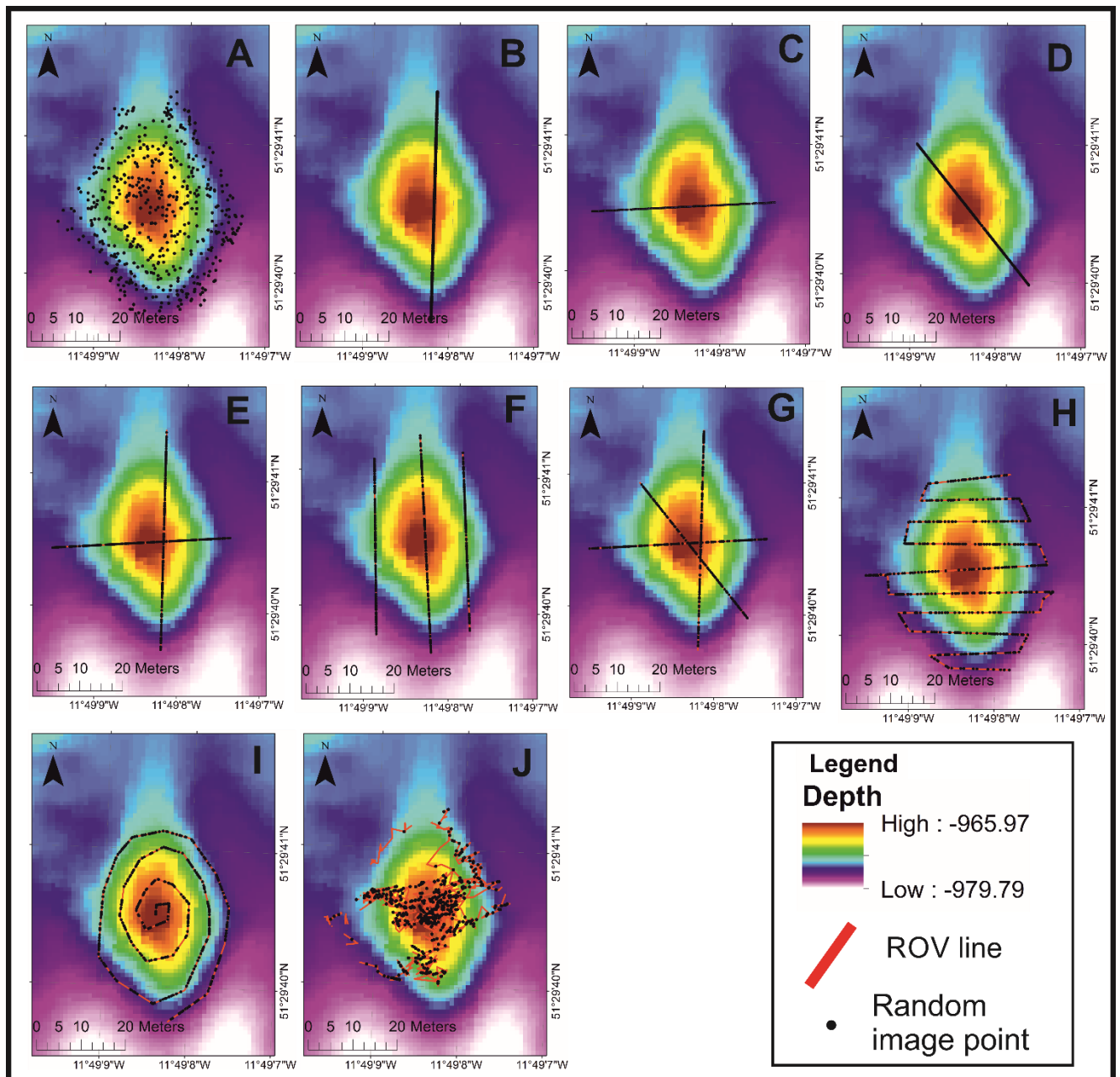


Figure 4 Video-survey designs facilitating the collection of X=510 random image points along the survey lines

A) random points (SD1), B) south-north transect (SD2), C) east-west transect (SD3), D) northwest-southeast diagonal transect (SD4), E) 2 lines (SD5), F) 3 straight, parallel line grid (SD6), G) 3 summit-crossing lines (SD7), H) horizontal grid (SD8), I) spiral (SD9) and J) an actual survey transect from a mound reconnaissance dive (SD10).

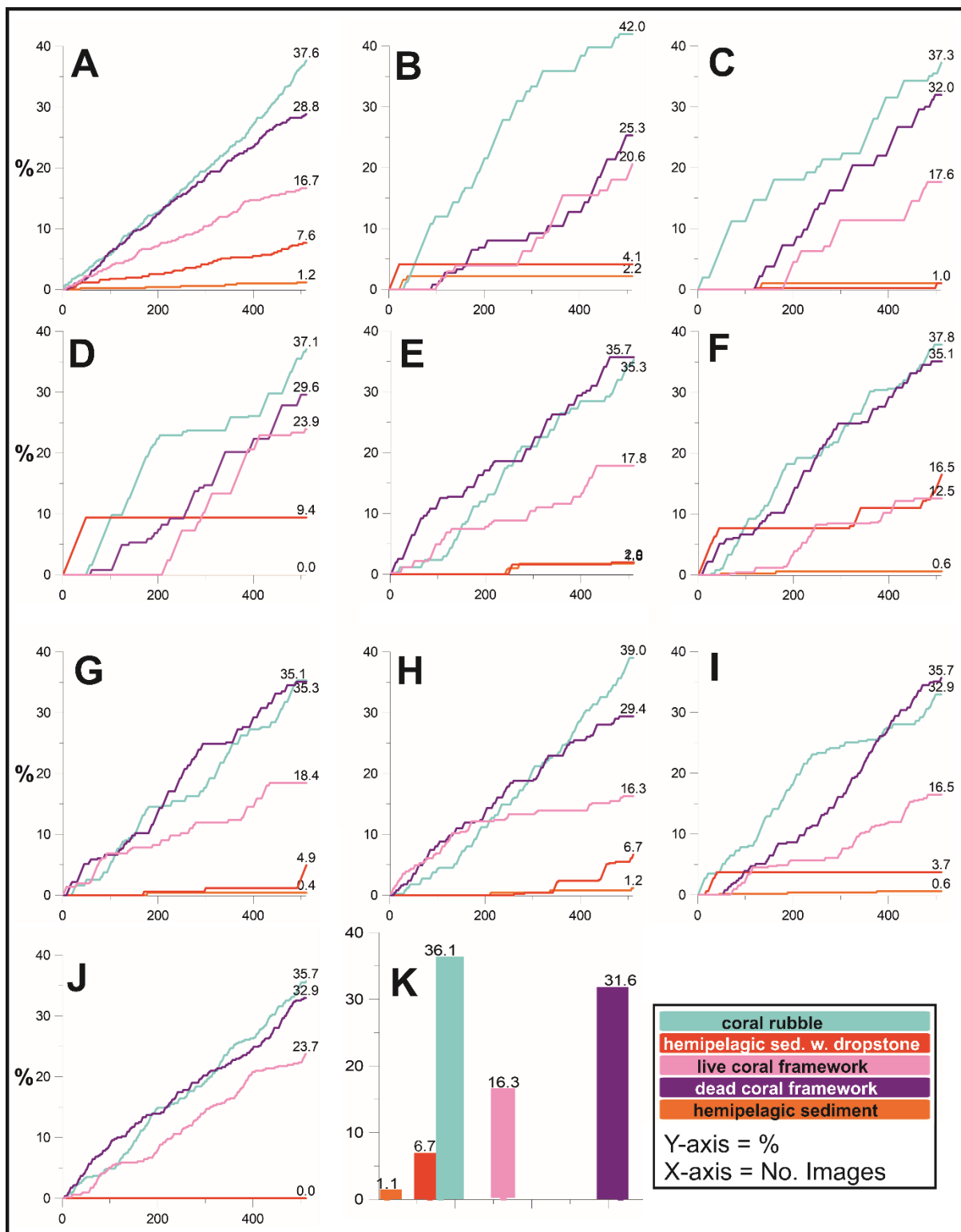
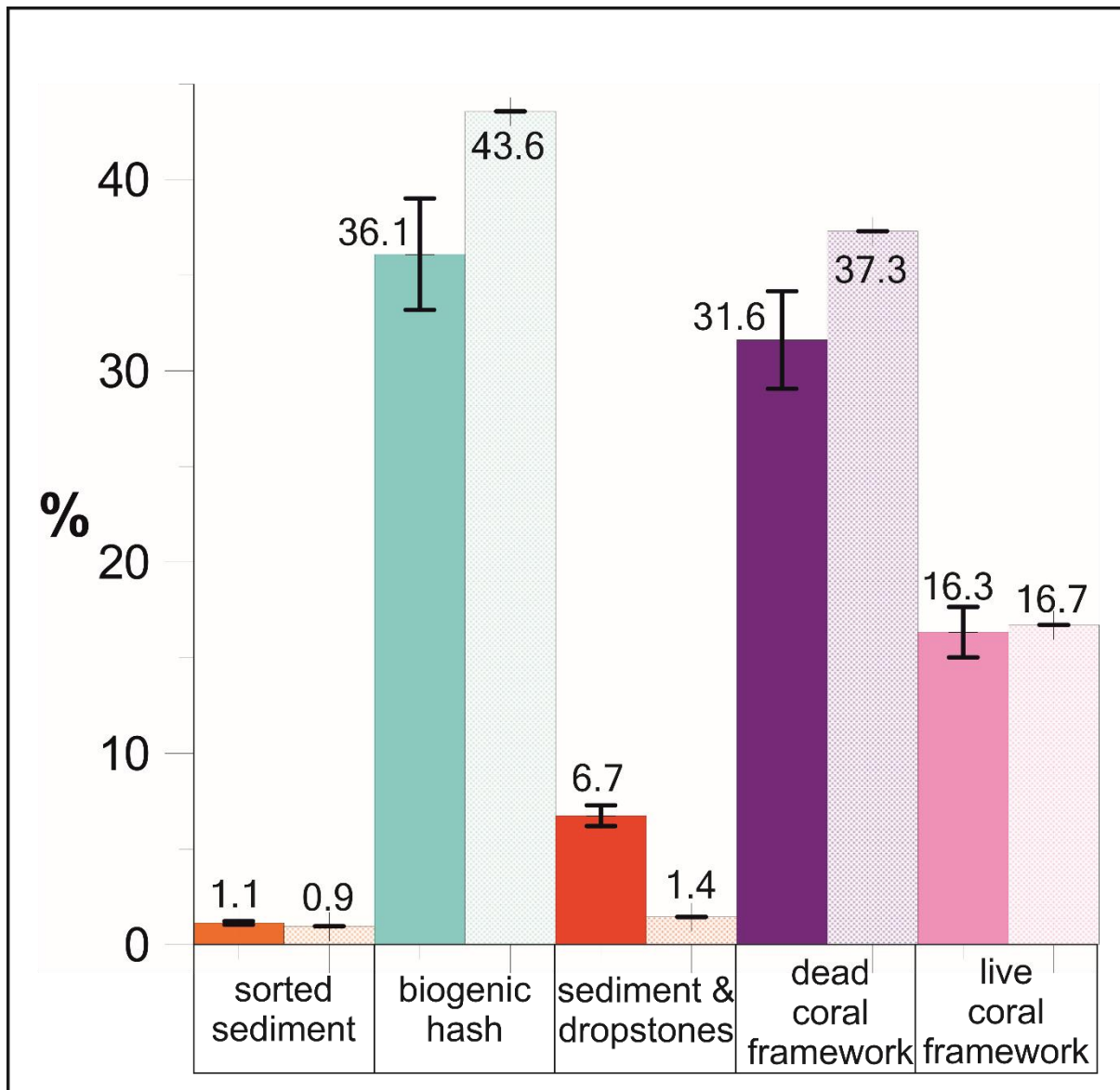


Figure 5 survey design results presented as facies sampling curves. A) random points (SD1), B) south-north transect (SD2), C) east-west transect (SD3), D) northwest-southeast diagonal transect (SD4), E) 2 lines (SD5), F) 3 straight, parallel line grid (SD6), G) 3 summit-crossing lines (SD7), H) horizontal grid (SD8), I) spiral (SD9), J) an actual survey transect from a mound reconnaissance dive (SD10) and K) single axis bar chart showing the total proportion of observed facies across the Piddington Mound. A) to J) y-axis=% percentage of facies, x-axis= number of images, K) y-axis=%

820



821

822

Figure 6 Graph comparing T1 and T4 facies.

823

824

T1 Piddington Mound cell-type proportions in checker fill. T4 Piddington Mound cell-type proportions in solid fill.

825

826

alpha (α)	($d^2 * n$)	m	$X = (n \text{ if } d = 0.05)$
0.5	0.44129	4	177
0.4	0.50729	4	203
0.3	0.60123	3	241
0.2	0.74739	3	299
0.1	1.00635	3	403
0.05	1.27359	3	510
0.025	1.55963	2	624
0.02	1.65872	2	664
0.01	1.96986	2	788
0.005	2.28514	2	915
0.001	3.02892	2	1212
0.0005	3.3353	2	1342
0.0001	4.11209	2	1645

827

828

Table 1 Minimum sample size estimation table after Thompson (1987)

829

Alpha values (α) represents the significance level which can be used to calculate the confidence level (e.g. an alpha of 0.05 gives a confidence level of 95%), d is the margin of error, n is the sample size, m is the minimum number of categories required (see Thompson (1987) for further details on m), X is sample size.

832

833

Class	Description	Typical Environment
hemipelagic sediment	cell dominated (>90 % cell coverage) by hemipelagic sediment i.e. sand or mud with no recognisable bioclasts or dropstones	no dropstones nor deposition of biogenic material. Potentially deposition of a sorted sediment under the influence of benthic currents.
coral rubble	cell dominated (>50 % cell coverage) by recognisable biogenic material (i.e. coral rubble, shell fragments) and sediment	deposition of mound-derived material
hemipelagic sediment with dropstones	cell dominated (>50 % cell coverage) by dropstones and sediment (sand or mud)	erosion, non-deposition or non-coral growth since the deposition of the dropstones
dead coral framework	cell dominated (>50 % cell coverage) by coral framework which has no identifiable living parts	coral no longer grows
live coral framework	cell dominated (>50 % cell coverage) by coral framework with identifiable living parts	coral growth

Table 2 Facies description

Class	T1_%	T4_%	Δ _%
hemipelagic sediment	1.14 (± 0.09)	0.96	-0.18
coral rubble	36.1 (± 3.14)	43.57	7.47
hemipelagic sediment with dropstones	6.74 (± 0.58)	1.45	-5.29
dead coral framework	31.61 (± 2.75)	37.3	5.69
live coral framework	16.38 (± 1.42)	16.72	0.34
no data	8	0	
Sum of classified cells	100.0	100.0	

Table 3 Comparison of T1 Piddington Mound cell-type proportions (T1_%) with T4 Piddington Mound proportions (T4_%).

The Δ _% column represents the percentage change between T1 and T4. All values are rounded up to the nearest two decimal places. Error margins are proportionally distributed from “no data” values.